ChemPubSoc Europe

DOI: 10.1002/chem.201804169

CHEMISTRY A European Journal Communication

Biochemistry

Discovery of Small Molecule WWP2 Ubiquitin Ligase Inhibitors

Jessica E. Watt,[a] Gregory R. Hughes,[a, c] Samuel Walpole,[b] Serena Monaco,[b] G. Richard Stephenson,[c] Philip C. Bulman Page,[c] Andrew M. Hemmings,[a, c] Jesus Angulo,*[b] and Andrew Chantry*[a]

Abstract: We have screened small molecule libraries specifically for inhibitors that target WWP2, an E3 ubiquitin ligase associated with tumour outgrowth and spread. Selected hits demonstrated dose-dependent WWP2 inhibition, low micromolar IC50 values, and inhibition of PTEN substrate-specific ubiquitination. Binding to WWP2 was confirmed by ligand-based NMR spectroscopy. Furthermore, we used a combination of STD NMR, the recently developed DEEP-STD NMR approach, and docking calculations, to propose for the first time an NMR-validated 3D molecular model of a WWP2-inhibitor complex. These first generation WWP2 inhibitors provide a molecular framework for informing organic synthetic approaches to improve activity and selectivity.

There are approximately 600 E3 ligases in the human genome, and they can be sub-divided into RING type and HECT domain ligases.[1] Within the HECT E3s is a small group (9 in total) referred to as the Nedd4 superfamily, which includes the WWP1, WWP2, Nedd4, ITCH and Smurf2 Ub ligases.[2] The 3D crystal structures have been resolved for the HECT domains within Nedd4,[3] WWP1,[4] and WWP2.[5,6] Accumulating evidence suggests that the Nedd4 ligases, and notably WWP1 and WWP2, are frequently mis-expressed in cancer.[7–9] Their overexpression in animal models causes increased tumour outgrowth,[10] and they also selectively control key oncogenic signaling events linked to both cancer initiation and spread.[11]

[a] J. E. Watt, G. R. Hughes, Dr. A. M. Hemmings, Dr. A. Chantry
School of Biological Sciences
University of East Anglia, Norwich NR4 7TJ (UK)
E-mail: a.chantry@uea.ac.uk

[b] S. Walpole, S. Monaco, Dr. J. Angulo
School of Pharmacy
University of East Anglia, Norwich NR4 7TJ (UK)
E-mail: j.angulo@uea.ac.uk

[c] G. R. Hughes, Dr. G. R. Stephenson, Prof. P. C. Bulman Page, Dr. A. M. Hemmings
School of Chemistry
University of East Anglia, Norwich NR4 7TJ (UK)

Supporting information and the ORCID identification number(s) for the author(s) of this article can be found under: https://doi.org/10.1002/chem.201804169.

There have been a number of recent attempts to develop HECT ligase inhibitors, and more specifically targeting the Nedd4 sub-family. Heclin was identified from a bicyclic peptide library screen and can selectively inhibit Smurf2, Nedd4 and WWP1 by inducing a conformational change that causes oxidation of the active site cysteine.[12] Chlomipramine emerged as a candidate ITCH ligase inhibitor based on an enzymatic assay-based high throughput screen and was shown to block both ITCH auto-ubiquitination and substrate-specific p73 ubiquitination, although IC50 values are in the low millimolar range.[13] Using a covalent tethering method, a new class of Nedd4 ligase inhibitors were identified and shown to react with a non-catalytic cysteine to hinder ubiquitin binding to this exosite and subsequent enzymatic processivity.[14] Additional attempts to discover Nedd4 inhibitors have utilised in silico modelling approaches supported by thermal shift binding experiments and revealed that derivatives of indole-3-carbinol may also bind to the processivity exosite in the Nedd4 catalytic HECT domain and inhibit substrate-specific ubiquitination linked to oncogenic signalling events.[15,16]

Here, we focused our efforts on developing small molecule inhibitors of the WWP2 ubiquitin ligase, an enzyme that can cause ubiquitin-dependent degradation of specific tumour suppressor proteins that are commonly lost in many types of cancer, namely Smad transcription factors, PTEN, and Oct4. To that aim, we have used high-throughput screening to identify hits from the *NCI Diversity Set V* and *NCI Approved Oncology Set V* small molecule libraries, we have confirmed binding to WWP2 by NMR spectroscopy, and used a combination of STD NMR, DiffErential EPitope mapping (DEEP)-STD NMR and docking calculations to generate for the first time an NMR-validated 3D molecular model of a WWP2-inhibitor complex. To discover first generation WWP2 ubiquitin ligase inhibitors we used a 96-well plate format high-throughput screen (HTS) using recombinant proteins and auto-ubiquitination as a readout for WWP2 activity (Figure 1 a).

Initially, to develop and optimise the HTS assay full-length WWP2 (WWP2-FL) expressed as a GST fusion protein in bacteria was attached onto glutathione-coated plates and then incubated with recombinant E1, E2 enzymes and Flag-tagged ubiquitin (Supporting Information Figure S1a). The specificity for WWP2 auto-ubiquitination was confirmed by detection of Ub-Flag conjugated WWP2 in the presence of all assay components and confirmed using a catalytically inactive WWP2-FL^{C838A} mutant (Supporting Information Figure S1b). Next, we used this assay to screen the *NCI Diversity Set V* and *NCI Approved*

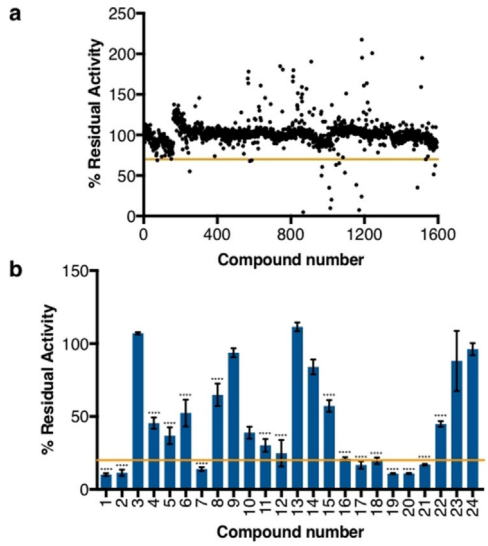

Figure 1. High throughput screen for WWP2 inhibitors. (a) HTS assays for NCI Diversity Set V were carried out using 10 μM compound at 0.1% DMSO in single shot with internal controls for 100% activity (DMSO) and 0% activity (E3 only) on each individual plate. All assays were normalised using 100% and 0% controls and had a threshold of 70% as indicated by the yellow line. $0.5 < Z' < 0.9$ for all single shot assays. (b) Auto-ubiquitination assay on 24 Diversity set V hits at 10 μM and 0.1% DMSO with a threshold set at 20% as indicated by the yellow line.

Oncology Set V small molecule libraries consisting of 1,593 and 450 compounds, respectively. The initial screens were run as single shot assays at a concentration of 10 μM and 0.1% DMSO, with Z′ values over 0.5 suggesting that these plate assays were robust. The controls for each library screen showed no significant difference between the buffer and E3 only controls and no significant effect was observed in the presence of DMSO (Supporting Information Figure S1c). Results were normalised using the high and low controls to calculate the percentage residual activity compared to the DMSO control. A threshold of 70% (>2 SD from the DMSO control mean) was used to determine which compounds would be selected for further testing. We identified 24 initial hits from the NCI Diversity Set V screen, but no hits emerged from the NCI Oncology set (Figure 1a and Supporting Information Figure S1d). Potential hits emerging from the single shot assays were then tested in triplicate under the same assay conditions and at 10 μM compound concentration, and 17 of the initial 24 hits demonstrated significant decrease in WWP2 activity (Figure 1b). These were then further ranked more stringently based on <20% residual activity thresholds, and further de-selected based on dose-dependent WWP2 inhibition (Supporting Information Figure S2). In total, 10 potential hit inhibitors with varied structural compositions were identified and the majority of these gave IC50 values in the low micromolar range (Supporting Information Table S1), and five of these inhibitors had IC50 values below 3 μM (Table 1).

We next further analysed all 10 selected hit compounds based on counter assays against E1, E2, Nedd4 and WWP1 ubiquitin ligases. Since the WWP2 auto-ubiquitination is dependent on prior sequential activation of ubiquitin by E1 and E2 ubiquitin ligases, we addressed whether any of the lead inhibitors were affecting this ubiquitin priming step earlier within in the auto-ubiquitination cascade. We therefore developed and optimised ubiquitination assays to measure UbcH7 (E2) and Uba1 (E1) activities. For UbcH7, we used a similar plate assay approach as used to measure E3 activity but used bacterially His-tagged UbcH7 and bound this protein onto nickel-coated 96-well plates. Once the assay was optimised to obtain significant 100% and 0% activity controls, compounds were tested at the same initial concentrations as used in the GST-WWP2-FL screening, and no significant decrease in activity was observed for all compounds in the His-E2 ubiquitination assay (Supporting Information Figure S3a). To assess compound effects on E1 activity, we used a different gel-based approach due to difficulties in developing robust and reproducible plate assays. Recombinant His-Uba1 and ubiquitin undergo E1-mediated transthiolation when incubated together and the formation of higher molecular weight mono-Ub-E1 conjugates was clearly apparent when separated by SDS-PAGE and stained with Coomassie Blue. In the presence of the WWP2 lead inhibitory compounds we found no discernible impact on E1 ubiquitin conjugation (Supporting Information Figure S3b). Hit compounds were next tested against Nedd4 and WWP1 to find out whether they were capable of inhibiting other HECT E3 ligases in the same family as WWP2. GST-tagged Nedd4 and His-tagged WWP1 were immobilised onto glutathione coated and nickel coated plates, respectively. Auto-ubiquitination levels were determined using HRP-conjugated anti-Flag antibody and TMB substrate. Both Nedd4 and WWP1 produced a significant increase in OD when in the presence of E1, E2, and ubiquitin, unlike all other reactions (Supporting Information Figure S3c).

There was no significant difference between reactions which lacked one or more components, showing that Nedd4 and WWP1 are capable of auto-ubiquitination under these assay conditions. All inhibitors tested demonstrated some degree of

Table 1. Summary of selected hits from WWP2 inhibitor screen and IC50 values. Data for STD-NMR and CPMG are included, and (?) indicates inconclusive data due to poor solubility and/or low signal/noise ratios.

Cpd./NSC	Structure	IC50 (μM)	STD-NMR	CPMG
1/2805	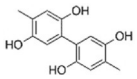	0.38	✓	✓
7/228155	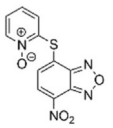	0.84	×	×
12/44750	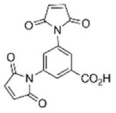	0.85	?	?
19/228150	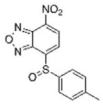	1.29	?	?
20/288387	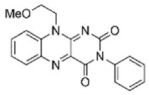	2.30	✓	✓

inhibition against all three E3 ubiquitin ligases, although several of the inhibitors tested were more potent against WWP2. Compounds **1**, **2** and **12** showed no significant difference between the HECT E3 ligases, implying that these compounds are not selective towards one of the ligases (Supporting Information Figure S3d). Nevertheless, these three compounds do show a significant reduction in activity for all three proteins. Compounds **7** and **19** showed a significant difference between WWP2 and WWP1, and WWP1 and Nedd4 but **7** and **19** presented no difference between WWP2 and Nedd4. Interestingly, compounds **16**, **17**, **18**, **20** and **21** showed increased inhibition towards WWP2 over WWP1 and Nedd4 (Supporting Information Figure S3d). We next tested for substrate-specific effects, and determined whether these inhibitors could affect WWP2-dependent PTEN ubiquitination. Reactions contained E1, E2, WWP2, PTEN, ubiquitin and ATP and were analysed by western blotting. In the presence of selected hit compounds representing a broad range of IC50 values based on the HTS assay, it is clear that each can robustly inhibit WWP2-dependent PTEN ubiquitination (Figure 2).

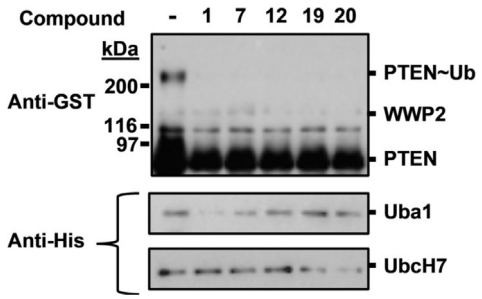

Figure 2. Effects of WWP2 inhibitors on substrate-specific PTEN ubiquitination. In vitro GST-PTEN ubiquitination reactions in the absence and presence of compounds, analysed using western blotting with anti-GST and anti-His antibodies.

Ligand-based NMR was then used to confirm binding of hit compounds to the WWP2 HECT catalytic domain. We used i), Saturation Transfer Difference (STD) NMR and ii), Carr–Purcell–Meiboom–Gill (CPMG) NMR experiments, two widely used techniques for lead screening in drug discovery.[17] STD NMR spectroscopy relies on protein-selective saturation being transferred only to the bound ligands in fast exchange with the receptor.[18,19] Hence, the presence of signals in the STD difference spectra of a sample containing one ligand (or more) in the presence of a receptor indicates binding. CPMG NMR experiments, also called T_2-filter experiments, rely on a filter (repeating spin-echo building blocks in the pulse sequence) whose aim is to eliminate the signals coming from large molecules (usually having a short transverse relaxation time, T_2).[20] Bound ligands transiently acquire a T_2 similar to that of the receptor, and so their signal will be filtered out as well. In the CPMG spectrum, the absence (or strong reduction) of ligand signals in the presence of a receptor indicates binding.

The NMR screening provided clear-cut results for six of the hit compounds, as shown by positive binding results in both the STD and CPMG NMR experiments (**1**, **2**, **16**, **17**, **18** and **20**, see Table 1, Supporting Information Table S1 and Figure S4). Compounds **12**, **19** and **21** were excluded as they showed very weak signals both in the binding experiments and in the control spectra, probably ascribable to solubility issues; while compound **7** showed no STD signals. It is important to highlight that fast exchange between the free and the bound state is an essential condition for STD NMR.[21] The STD signal is detected in the ligand free state; if the ligand resides within the binding pocket for a long period of time, the saturation is not sufficiently accumulated during the saturation time. The low IC50 value determined for compound **7** (0.84 μM) and the absence of STD signals for this hit could indicate too strong an affinity of binding. This would make compound **7** unsuitable for ligand-based NMR observation, but the results do not necessarily exclude it as a binder.

STD NMR has also great potential in structurally elucidating the binding mode of a ligand in complex with the protein at atomic detail, providing the binding epitope mapping of the ligand.[21] Among the six identified binders based on STD-NMR data, we selected NSC288387 (compound **20**) since it showed the clearest STD signals (probably as a consequence of its mid-range IC50, of 2.30 μM) to deepen the structural analysis by performing STD binding epitope mapping. The STD binding epitope mapping (Figure 3a) suggests that the main recognition element in the complex between WWP2 HECT and compound **20** is the unsubstituted *N*-phenyl ring (labelled B in Figure 3); ring A and the aliphatic ether adjacent to it show weaker interactions, suggesting that this part of the molecule would be the most solvent exposed.

We then used computational techniques to identify the binding site on the WWP2 HECT domain (based on the PDB ID: 4Y07[5]) and to then dock compound **20** into the putative binding pocket (see Supporting Information Table S2 and Figure 3b). The lowest energy docking solution, shown in Figure 3b (see also Supporting Information Table S2), was in very good agreement with the binding epitope experimentally determined by STD NMR. Furthermore, as a step further for the

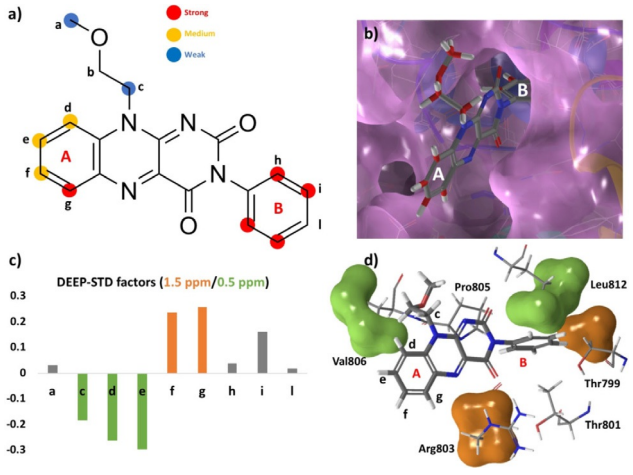

Figure 3. Differential epitope mapping of compound 20 (NSC288387) in complex with WWP2-HECT domain. a) STD Binding epitope mapping, b) lowest energy docking solution of NSC288387 onto WWP2 HECT domain, c) DEEP-STD factors (1.5 ppm/0.5 ppm) and d) details of the binding pocket for NSC288387. In d), residues within 5 Å from the ligand are shown, protein protons resonating at 0.5 ppm and 1.5 ppm are enclosed in a green and orange surface, respectively (see also Supporting Information Table S5).

validation of the 3D model of the complex, we employed the newly developed DEEP-STD NMR approach (relying on protein irradiation at differential frequencies) which allows the identification of the types of amino-acids lining the binding pocket that make inter-molecular contacts with specific single protons of the ligand.[22] The DEEP-STD NMR data obtained by differential irradiation of the protein at 0.50 and 1.50 ppm (Figure 3c) provided additional experimental support for the 3D molecular model of the complex generated by the docking approach. Frequencies 0.50 and 1.50 ppm correspond to methyl groups of valine and isoleucine, and the arginine β/γ protons, respectively (see Supporting Information Table S3 and S4). Closer inspection of the docking solution in the putative binding pocket reveals the presence of Val806 and Arg803 at close distances from ring A of the ligand (Figure 3d and Supporting Information Table S5).

Remarkably, the docking solution structure shows ligand protons c, d and e pointing towards the methyl group of Val806, and protons f and g, pointing towards the Arg803, on the opposite side of the binding pocket. This is in perfect agreement with the DEEP-STD factors (1.5/0.5 ppm) observed for these protons (Figure 3c): protons c, d and e show negative DEEP-STD factors, and protons f and g show positive DEEP-STD factors (suggesting vicinity with protein residues resonating at 0.5 and 1.5 ppm, respectively). The excellent match between the docking solution of compound **20** in the putative binding pocket and the pharmacophore of both the ligand and the binding site (obtained by STD NMR and DEEP-STD NMR, respectively) give us solid ground to propose the model as the first 3D structure of a WWP2 inhibitor bound to its target (Figure 3 and Supporting Information Figure S5). Furthermore, this NMR-validated model is supported by molecular dynamics simulation studies demonstrating stability of the complex (Supporting Information Figures S6–S8).

In summary, the compounds discovered in this study represent the first generation of WWP2 ubiquitin ligase inhibitors. Additionally, through a combination of HTS, ligand-based NMR, DEEP-STD NMR and docking calculations we have been able to propose for the first time a 3D molecular model of a WWP2-inhibitor complex. Collectively, these data provide a framework for developing new classes of ubiquitin ligase inhibitors that can progress through further organic synthesis to improve compound activity and specificity and have potential to generate lead therapeutic compounds. We are currently working towards unravelling the mechanism of inhibition by these novel ligands and further probing the ligand binding sites using combined DEEP-STD NMR and crystallography approaches. We anticipate that, building up from this work, subsequent lead optimization will provide novel analogues that can progress through to potential therapeutic compounds.

Acknowledgements

The work was supported by funding to A.C. from Prostate Cancer UK supporting a PhD Studentship for J.W. through Research Grant S13-007, and funding to A.C. from James Tudor Foundation. G.H. was supported by a Biotechnology and Biological Sciences Research Council (BBSRC) iCASE PhD Studentship awarded to A.C. and P.B.P. in collaboration with Charnwood Molecular Ltd. S.M. acknowledges a PhD Studentship from the School of Pharmacy at the University of East Anglia (UEA). J.A. and S.W. received funding from the BBSRC through Research Grant BB/P010660/1 and a DTP-PhD Studentship, respectively. We thank Dr. Tharin Blumenschein from the School of Chemistry at UEA for helpful discussions.

Conflict of interest

The authors declare no conflict of interest.

Keywords: DEEP-STD NMR · drug discovery · ubiquitin ligase · inhibitors · saturation transfer difference NMR

[1] W. Li, M. H. Bengtson, A. Ulbrich, A. Matsuda, V. A. Reddy, A. Orth, S. K. Chanda, S. Batalov, C. A. P. Joazeiro, *PLoS ONE* **2008**, *3*, e1487.
[2] S. Soond, A. Chantry, *Bioessays* **2011**, *33*, 749.
[3] E. Maspero, S. Mari, E. Valentini, A. Musacchio, A. Fish, S. Pasqualato, S. Polo, *EMBO Rep.* **2011**, *12*, 342.
[4] M. A. Verdecia, C. A. Joazeiro, N. J. Wells, J. L. Ferrer, M. E. Bowman, T. Hunter, J. P. Noel, *Mol. Cell* **2003**, *11*, 249.
[5] W. Gong, X. Zhang, W. Zhang, J. Li, Z. Li, *Acta Crystallogr. Sect. F* **2015**, *71*, 1251.
[6] Z. Chen, H. Jiang, W. Xu, X. Li, D. R. Dempsey, X. Zhang, P. Devreotes, C. Wolberger, L. Mario Amzel, S. B. Gabelli, P. A. Cole, *Mol. Cell* **2017**, *66*, 345.
[7] E. Cerami, J. Gao, U. Dogrusoz, B. E. Gross, S. O. Sumer, B. A. Aksoy, A. Jacobsen, C. J. Byrne, M. L. Heuer, E. Larsson, Y. Antipin, B. Reva, A. P. Goldberg, C. Sander, N. Schultz, *Cancer Discov.* **2012**, *2*, 401.
[8] S. M. Soond, P. G. Smith, L. Wahl, T. E. Swingler, I. M. Clark, A. M. Hemmings, A. Chantry, *Biochim. Biophys. Acta Mol. Basis Dis.* **2013**, *1832*, 2127.
[9] X. Zou, G. Levy-Cohen, M. Blank, *Biochim. Biophys. Acta* **2015**, *1856*, 91.
[10] S. Maddika, S. Kavela, N. Rani, V. R. Palicharia, J. L. Pokorny, J. N. Sarkaria, J. Chen, *Nat. Cell Biol.* **2011**, *13*, 728.
[11] A. Chantry, *Cell Cycle* **2011**, *10*, 2437.
[12] T. Mund, M. J. Lewis, S. Maslen, H. R. Pelham, *Proc. Natl. Acad. Sci. USA* **2014**, *111*, 16736.
[13] M. Rossi, B. Rotblat, K. Ansell, I. Amelio, M. Caraglia, G. Misso, F. Bernassola, C. N. Cavasotto, R. A. Knight, A. Ciechanover, G. Melino, *Cell Death Dis.* **2014**, *5*, e1203.
[14] S. G. Kathman, I. Span, A. T. Smith, Z. Xu, J. Zhan, A. C. Rosenzweig, A. V. Statsyuk, *J. Am. Chem. Soc.* **2015**, *137*, 12442.
[15] I. Aronchik, A. Kundu, J. G. Quirit, G. L. Firestone, *Mol. Cancer Res.* **2014**, *12*, 1621.
[16] J. G. Quirit, S. N. Lavrenov, K. Poindexter, J. Xu, C. Kyauk, K. A. Durkin, I. Aronchik, T. Tomasiak, Y. A. Solomatin, M. N. Preobrazhenskaya, G. L. Firestone, *Biochem Pharmacol.* **2017**, *127*, 13.
[17] M. Pellecchia, I. Bertini, D. Cowburn, C. Dalvit, E. Giralt, W. Jahnke, T. L. James, S. W. Homans, H. Kessler, C. Luchinat, C. B. Meyer, H. Oschkinat, J. Peng, H. Schwalbe, G. Siegal, *Nat. Rev. Drug Discovery* **2008**, *7*, 738.
[18] J. Angulo, P. M. Nieto, *Eur. Biophys. J.* **2011**, *40*, 1357.
[19] M. Mayer, B. Meyer, *Angew. Chem. Int. Ed.* **1999**, *38*, 1784 – 1788; *Angew. Chem.* **1999**, *111*, 1902 – 1906.
[20] S. Meiboom, D. Gill, *Rev. Sci. Instrum.* **1958**, *29*, 688.
[21] M. Singh, B. Tam, B. Akabayov, *Molecules* **2018**, *23*, 233.
[22] S. Monaco, L. E. Tailford, N. Juge, J. Angulo, *Angew. Chem. Int. Ed.* **2017**, *56*, 15289; *Angew. Chem.* **2017**, *129*, 15491.

Manuscript received: August 15, 2018
Accepted manuscript online: September 12, 2018
Version of record online: November 6, 2018

